Characterization of Three-Dimensional Open Dielectric Structures Using the Finite-Difference Time-Domain Method

Nihad Dib, *Member, IEEE,* and Linda P. B. Katehi, *Fellow, IEEE*

Abstract— **Millimeter and submillimeter wave three-dimensional (3-D) open dielectric structures are characterized using the finite-difference time-domain (FDTD) technique. The use of FDTD method allows for the accurate characterization of these components in a very wide frequency range. The first structure characterized through FDTD for validation purposes is a mm-wave image guide coupler. The derived theoretical results for this structure are compared to experimental data and show good agreement. Following this validation, a sub-mm wave transition from a strip-ridge line to a layered ridge dielectric waveguide (LRDW) in open environment is analyzed, and the effects of parasitic radiation on electrical performance are studied. The transition is found to be very efficient over a wide sub-mm frequency band which makes it useful for a variety of applications. In addition to the transition, a sub-mm wave distributed directional coupler made of the LRDW is extensively studied using the FDTD method as an analysis tool. Furthermore, an iterative procedure based on the FDTD models is used to design a 3-dB coupler with a center frequency of 650 GHz and negligible radiation loss. This successful design shows that the FDTD technique can be used not only as an analysis method, but also as a design tool to provide designs which take into account all high frequency parasitic effects.**

I. Introduction

RECENTLY, Engel and Katehi [1] suggested the development of monolithic sub-mm guiding structures that can be realized by considering variations of the early dielectric lines. The new waveguides are made of materials which are available in monolithic technology so that they are compatible with solid-state sources (see Fig. 1). The dimensions of these monolithic guides are fractions of a guided wavelength, so the new structures may be used not only as guiding media but as means of making passive components. Presently, limitations in the fabrication process and availability of III-V materials permit use of these lines only at the high frequency end of the sub-mm wave spectrum.

The successful use of dielectric lines in a hybrid or monolithic environment relies mainly on the ability to realize an efficient transition to the dielectric waveguide. In the past, a variety of transitions from rectangular waveguide to mm-wave dielectric lines have been mainly characterized experimentally [2], [3]. When layered ridge dielectric waveguides (LRDW's) [1] are used in a monolithic environment, transitions to and out of dielectric waveguide may be realized through a short length of printed conductor line on top of the ridge (Fig. 2) [4]. In this manner, the dielectric waveguide components are effectively coupled to other conventional monolithic circuit components which are printed on the same wafer. Previous work on the characterization of such a transition exclusively considered the transition operating in an ideal shielding environment which was designed to effectively shield only that circuit component. As a result, the cavity was chosen adequately small enough and it was placed far enough from the transition so that it did not resonate within the frequency band and did not interfere with the circuit. The electrical performance of this ideal transition was analyzed by a hybrid full-wave integral equation-mode matching (IEMM) analysis technique and preliminary results were presented in [5]. Furthermore, a detailed study of the same shielded transition, using both the IEMM and finite-difference time-domain (FDTD) methods, is presented in [4]. In practice, however, monolithic circuits operate in open environments or within larger shielding packages and may suffer from parasitic radiation (space and surface waves losses) which limits performance considerably and intensifies unwanted electromagnetic interference between circuit components. As a result, parasitic radiation needs to be studied carefully and should be accounted for during design. In response to this need, this paper addresses the issue of parasitic radiation by a microstrip-to-dielectric waveguide transition operating in an open environment. The performance of this transition is computed using the FDTD technique and the effects of parasitic radiation on the transition performance are discussed.

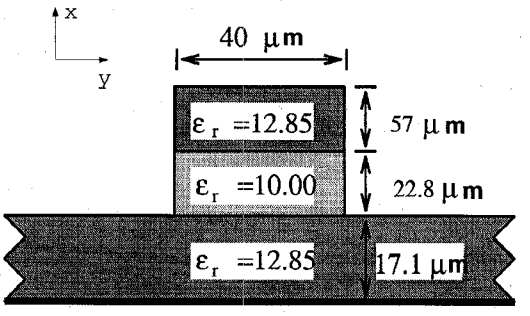

Fig. 1. Cross section of the layered ridge dielectric waveguide (LRDW) structure under study.

Manuscript received October 17, 1994; revised December 18, 1995. This work was supported by Rome Laboratory, Hanscom AFB Contract # F19628-92-K-0027 and by the Army Research Office.

The authors are with the Radiation Laboratory, University of Michigan, Ann Arbor, MI 48109–2122 USA.

Publisher Item Identifier S 0018-9480(96)02348-4.

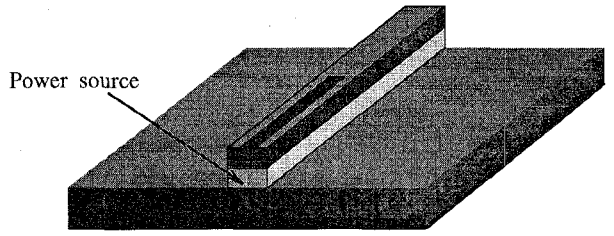

Fig. 2. A transition between a power source and a LRDW through a strip-ridge line.

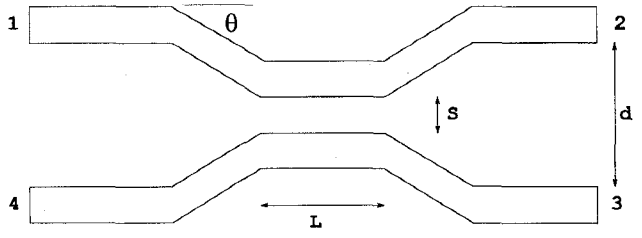

Fig. 3. Top view of a distributed directional coupler.

The second half of this work is devoted to the dielectric waveguide coupler. The distributed directional coupler, shown in Fig. 3, which consists of a section of a coupled dielectric guide of length L and separation S, presents the simplest coupler geometry. Such a coupler can be made of any type of dielectric waveguide and has been the subject of study of many publications (see, e.g., [6]–[8]). In most of these studies the coupler design was completed by choosing the appropriate coupling length through empirical formulas for the magnitudes of S_{12} and S_{13}. This approach, however, neglects interference between the feeding lines as well as radiation loss which can be substantial in open dielectric waveguides [9] and predicts performances which are unrealizable. To overcome this problem, when comparing experimental and theoretical results, measured data had to be normalized accordingly, to numerically eliminate the effect of the dielectric and radiation losses at the bends and junctions [7], [8]. This work revisits the open dielectric waveguide coupler problem in an effort to understand the effects of parasitic radiation on coupler performance and account for these effects in design. The FDTD technique is used to analyze the coupler geometry and simulate the open environment in which the coupler operates by appropriate absorbing boundary conditions. For validation purposes, a mm-wave coupler which utilizes the image guide is analyzed first, and compared to experimental data. Following this validation, a sub-mm wave directional coupler made of the LRDW, shown in Fig. 1, is extensively studied. The scattering parameters and radiation loss factor of both couplers are presented.

II. Theory

The FDTD method is well known [10] and thus will not be presented here. In order to excite the dielectric waveguide, the vertical electric field component at the front plane ($z = 0$) is excited (see Fig. 4) and the magnetic wall source condition of [11] is used to compute the fields elsewhere in the plane $z = 0$. The source distribution has been modified to take into account the discontinuity experienced by the vertical electric field [12]. The incident field has a time variation given by a Gaussian envelope imposed on a sinusoidally varying carrier [13]. The space steps, $\Delta x, \Delta y$, and Δz, are carefully chosen such that integral numbers of them can approximate the various dimensions of the structure. For the LRDW structures under study, the following parameters are used: $\Delta x = 5.7\,\mu$m, $\Delta y = \Delta z = 10\,\mu$m, and $\Delta t = 0.014$ ps. The super-absorbing first-order Mur boundary condition [14] is used at the front and back walls in order to simulate infinite lines. On the other hand, the first-order Mur boundary condition is used on the top and side walls. For the LRDW under study, the left and right absorbers were placed at a distance of $240\,\mu$m from the edges of the ridge, while the top absorber was placed at a distance of $300\,\mu$m from the top surface of the ridge.

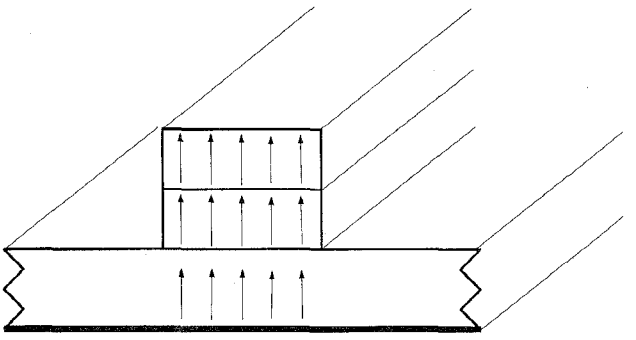

Fig. 4. Excitation for the dielectric waveguide.

III. Results and Discussion

A. Strip-Ridge to LRDW Transition

Of primary interest in evaluating the performance of the the transition shown in Fig. 2 is the power transferred from the dominant mode in the strip-ridge structure to the dominant mode in the LRDW. Fig. 5 shows the magnitude of the reflection coefficient for this transition in the frequency range dc-550 GHz. Due to the fact that the strip-to-dielectric ridge waveguide transition is an open structure, the magnitude of S_{11} is always less than 1.0 even for frequencies below the waveguide dominant mode cutoff frequency (around 350 GHz) while the shielded transition showed a total reflection ($|S_{11}| = 1$) in [4]. Specifically, in the open transition, for operating frequencies between 100 and 300 GHz almost 20% of the incident power is lost in the form of space and surface waves which will be referred to as radiation loss in this paper. As the operating frequency approaches 500 GHz however, the return loss reduces to less than -10 dB for all frequencies from 500 to 570 GHz, where 570 GHz is the cutoff frequency of the first higher-order mode of the strip-ridge line. It is worth mentioning that the cutoff frequency of the first higher-order mode of the LRDW is around 690 GHz.

B. Directional Couplers

A simple design of the dielectric directional coupler shown in Fig. 3 assumes zero loss, negligible coupling due to the feeding dielectric waveguides and the tapered sections and

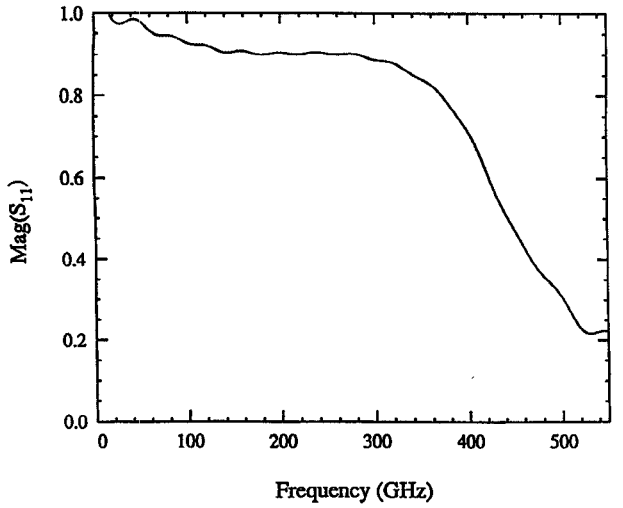

Fig. 5. Magnitude of S_{11} for the strip-ridge to LRDW transition.

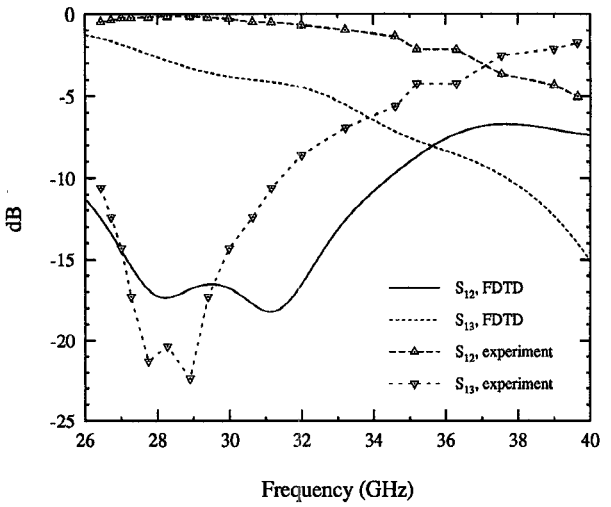

Fig. 6. Magnitudes of S_{12} and S_{13} of the image guide coupler compared to the experimental results from [2]. $S = 2.4$ mm, image guide width = 4.8 mm, image guide height = 2.4 mm, $\epsilon_r = 2.22$, $L = 59$ mm, $\theta = 26°$, and $d = 96$ mm.

considers quasi-static interactions in the coupling region. As a result, the magnitudes of the scattering parameters S_{12} and S_{13} can be obtained from the following relations [6], [8]

$$|S_{12}| = \left|\cos\left(\frac{\beta_e - \beta_o}{2}L\right)\right| \tag{1}$$

$$|S_{13}| = \left|\sin\left(\frac{\beta_e - \beta_o}{2}L\right)\right| \tag{2}$$

where β_e and β_o are the even and odd propagation constants of the coupled dielectric waveguide, respectively. With the knowledge of β_e and β_o, the coupling length L can be chosen to provide a coupler with a specific coupling coefficient $|S_{13}|$. An improvement of such an "ideal" design can be achieved by extending the effective coupling region within the tapered sections resulting in a modified version of (1) and (2) which include an effective coupling length, instead of the physical length, as suggested in [6]. The effective coupling length can be defined as

$$L_{\text{eff}} = L + \frac{\Delta\phi}{\beta_e - \beta_o} \tag{3}$$

$$\Delta\phi = 2\int_{z_0}^{z'} [\beta_{ze}(z) - \beta_{zo}(z)]\, dz \tag{4}$$

where the integration is performed along the axial direction of the coupler. z_0 corresponds to the junction between the coupled guide and the connecting arm, while z' is chosen to be some value of z beyond which the coupling between the arms is negligible. Due to the assumed "ideal" conditions of operation, (1) and (2) cannot account for any loss in the coupler. In the following sections, these ideal designs will be applied to the design of several submillimeter-wave couplers and their predicted coupler geometries will be analyzed by the FDTD technique. The predicted and numerically derived results will be compared in an effort to understand the effect of radiation loss on the coupler performance. Preceeding this study, the FDTD method is applied to analyze a 3-dB mm-wave image guide coupler which has been designed and successfully realized by Solbach [15] in order to validate the FDTD code which will be used in this study.

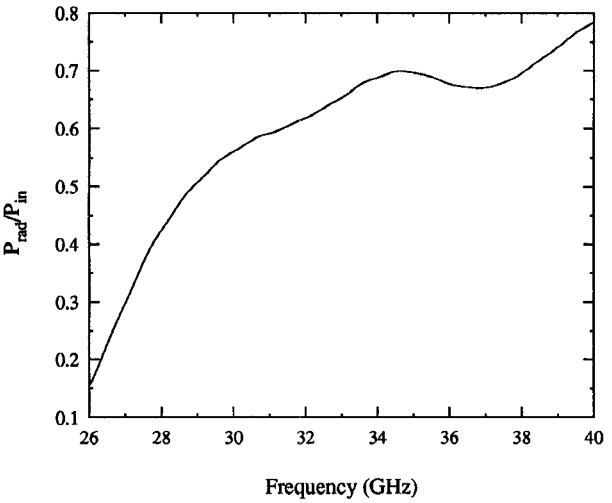

Fig. 7. Radiation loss factor $(1 - |S_{11}|^2 - |S_{12}|^2 - |S_{13}|^2 - |S_{14}^2|)$ of the image guide coupler.

As a first example, and for validation purposes, a distributed coupler made of image dielectric line is investigated. Fig. 6 shows $|S_{12}|$ and $|S_{13}|$ of the image guide coupler compared to the experimental results from [15]. Considering the fact that the experimental results were obtained through an implicit measurement with the assumption that the coupler is lossless, qualitative agreement between theory and experiment is satisfactory. The magnitude of S_{11} is found to be less than -30 dB in the whole frequency range which agrees with the experimental results in [15]. Fig. 7 shows the amount of radiated power from such a coupler which further verifies that radiation losses can not be neglected. It is worth mentioning that the FDTD obtained frequency at which $|S_{12}|$ and $|S_{13}|$ intersect agrees very well with that obtained using (1) and (2) in conjunction with (3) and (4) (see Fig. 13 in [15]). It should be mentioned that the tapered sections of the dielectric guide are modeled using the "staircase" approximation.

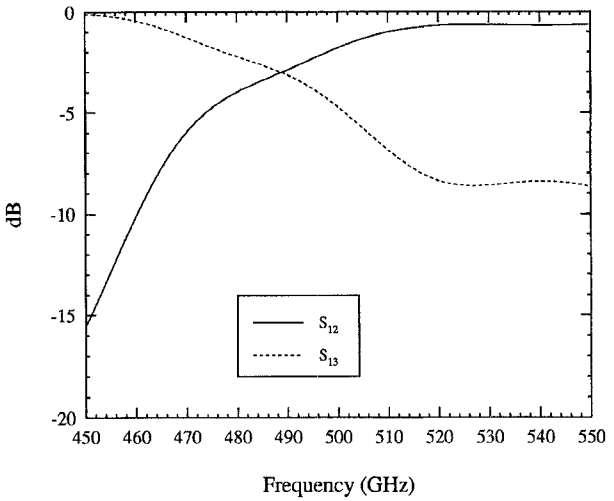

Fig. 8. Scattering parameters of an "ideal" LRDW coupler computed using (6) and (7) $S = 160\,\mu$m, $L = 870\,\mu$m.

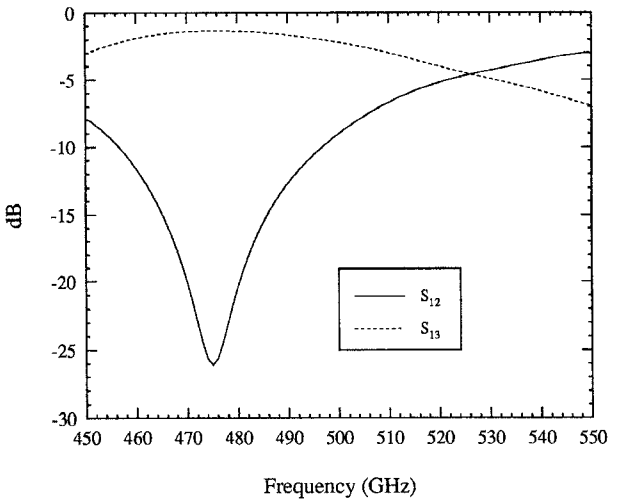

Fig. 9. Scattering parameters of the LRDW coupler obtained using the FDTD technique. $S = 160\,\mu$m, $L = 870\,\mu$m, $d = 320\,\mu$m, $\theta = 26^o$.

1) LRDW Coupler with $S = 160\,\mu$m: Having verified the developed 3-D FDTD code (see also [4], [16]–[18]) a sub-mm wave distributed directional coupler which employs the LRDW shown in Fig. 1 is studied. As a first example, an LRDW coupler with separation distance S of $160\,\mu$m and length L chosen such that a 3-dB coupler is obtained with a center frequency of 490 GHz is investigated. The scattering parameters of such a coupler obtained using (1) and (2) are shown as a function of frequency in Fig. 8. The same scattering parameters have been computed using the FDTD technique and are shown in Fig. 9. The sources of the discrepancy between the simulated results shown in Fig. 9 and the "ideal" response shown in Fig. 8 are the effects of the junctions and the coupling between the connecting guides. From a comparison between the "ideal" prediction and the FDTD results, we can see a shift in the design frequency by 7%. Specifically, as indicated by the FDTD analysis, the "ideal" design has resulted in a "nearly" 3-dB coupler at 525 GHz which is 35 GHz higher than the design frequency. Furthermore, due to parasitic radiation, $|S_{12}|$ and $|S_{13}|$ are -4.3 dB at the intersection point instead of -3 dB. In relation to this observation, Fig. 10 shows radiation loss as predicted by the FDTD method. From this figure, it can be seen that at 490 GHz, almost 25% of the input power is lost as parasitic radiation in the form of space and surface waves. It should be mentioned that $|S_{11}|$ and $|S_{14}|$ have been found to be less than -15 dB in the frequency range 450–550 GHz.

A slightly better design is obtained by the "modified ideal equations." Specifically, Fig. 11 shows the scattering parameters obtained using (1) and (2) in conjunction with (3) and (4) and clearly indicates a frequency shift of the center frequency by approximately 25 GHz from the design frequency. In this figure, the coupling in the straight connecting guides in addition to the tapered sections has been taken into account.

2) LRDW Coupler with $S = 40\,\mu$m: Another coupler with a separation distance $S = 40\,\mu$m has been also studied. Using (1) and (2), the length L is chosen such that a 3 dB-coupler is obtained with a center frequency of 600 GHz. The

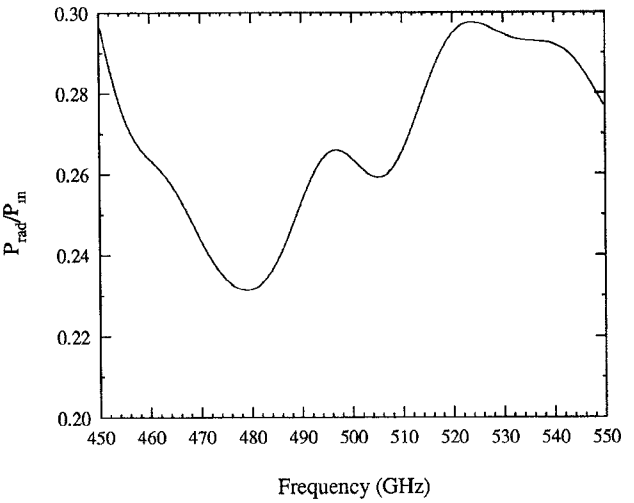

Fig. 10. Radiation loss factor of the LRDW coupler. $S = 160\,\mu$m, $L = 870\,\mu$m, $d = 320\,\mu$m, $\theta = 26^o$.

scattering parameters of such a coupler obtained using these two equations are shown in Fig. 12. The scattering parameters and the radiation loss factor for the same coupler obtained using the FDTD technique are shown in Figs. 13 and 14. After extensive numerical experiments on couplers with different coupling and tapered sections lengths, but with the same separation distance of $40\,\mu$m, low radiation loss around 630 GHz has been systematically observed. It should be mentioned that the radiation loss of the previous coupler with $S = 160\,\mu$m had a minimum around 480 GHz and was greater than 0.26 for frequencies above 550 GHz though not shown in Fig. 10. This suggests that the low radiation loss phenomenon around 630 GHz is a result of the separation distance and the cross section of the single LRDW itself. The magnitudes of S_{11} and S_{14} for this coupler are less than -18 dB in the frequency range 550–650 GHz but are not shown here. As observed in the previous example, the center frequency has clearly shifted upwards. The scattering parameters obtained using the

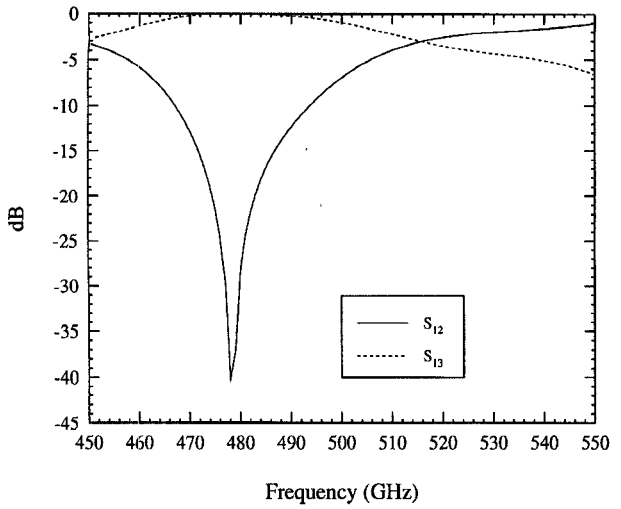

Fig. 11. Scattering parameters of the LRDW coupler obtained using the "modified ideal" equations. $S = 160\,\mu$m, $L = 870\,\mu$m, $d = 320\,\mu$m, $\theta = 26^o$.

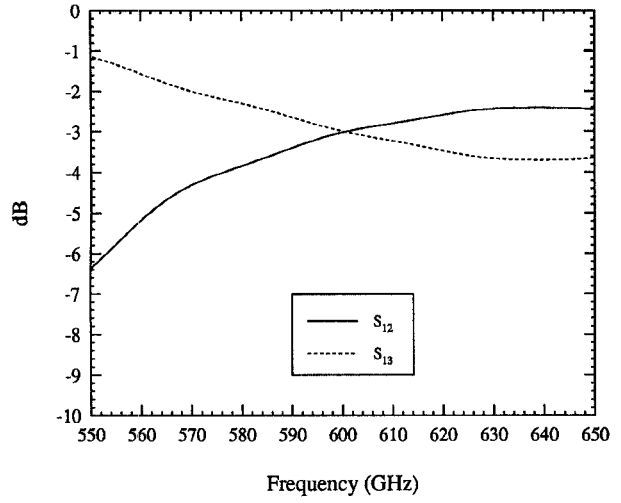

Fig. 12. Scattering parameters of an "ideal" LRDW coupler computed using (6) and (7). $S = 40\,\mu$m, $L = 180\,\mu$m.

"modified ideal" equations are also included in Fig. 13 and clearly indicate a frequency shift of the center frequency. The magnitude of S_{12} derived by FDTD and the "modified ideal" method agree well for frequencies larger than 600 GHz because of the low radiation loss at these frequencies.

Having noticed the fact that the actual center frequency is always larger than the design frequency due to the effect of the junctions, the FDTD code was executed for several coupling lengths with the separation distance $S = 40\,\mu$m. Figs. 14 and 15 show the radiation loss and the scattering parameters of the coupler with a coupling length $L = 80\,\mu$m obtained using the FDTD technique. The point of intersection between $|S_{12}|$ and $|S_{13}|$ occurs at 650 GHz with a value of -3.2 dB. It is interesting to see that the radiation loss at the center frequency is negligible. As before, $|S_{11}|$ and $|S_{14}|$ are less than -14 dB for the whole frequency range. Thus, with the coupling length of 80 μm, a 3-dB coupler may be realized with a center frequency of 650 GHz.

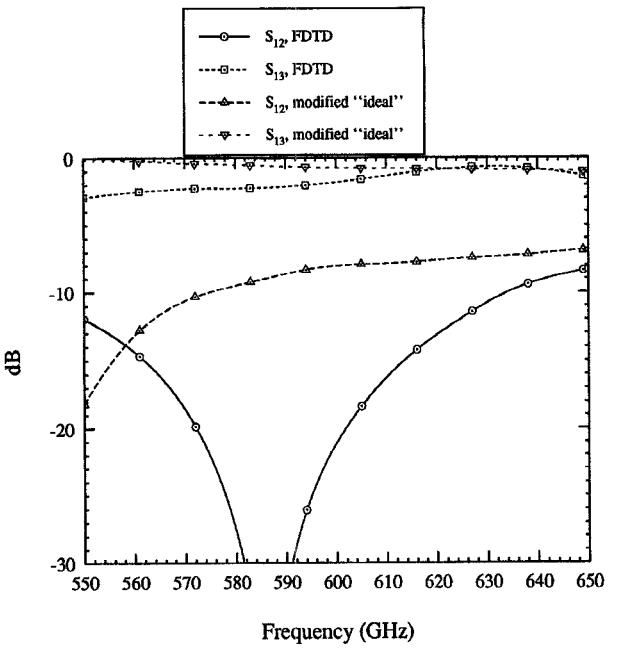

Fig. 13. Scattering parameters of the LRDW coupler obtained using FDTD. $S = 40\,\mu$m, $L = 180\,\mu$m, $d = 320\,\mu$m, $\theta = 26^o$.

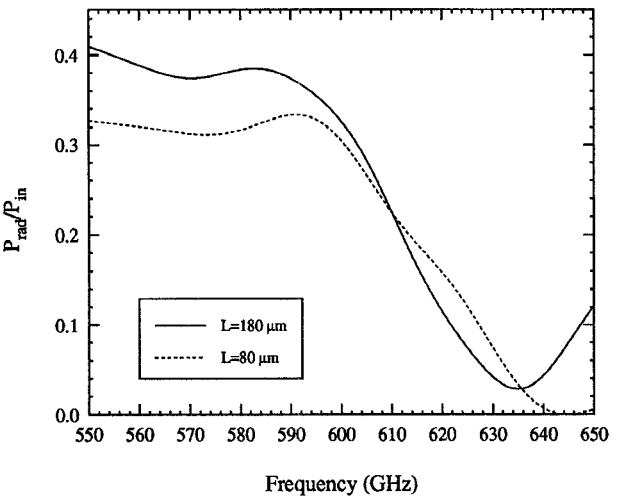

Fig. 14. Radiation loss factor of the LRDW coupler. $S = 40\,\mu$m, $d = 320\,\mu$m, $\theta = 26^o$.

IV. Conclusion

The FDTD method has been used to analyze three-dimensional mm- and sub-mm-wave dielectric waveguide structures. At first, a sub-mm wave transition from a strip ridge line to a LRDW has been studied. The transition has been found to be effective for frequencies above 500 GHz. Following this, an image line coupler has been characterized, for validation purposes, and the FDTD results were compared with experimental data. It has been found that the radiation loss cannot be neglected in such a structure. Following this validation, a sub-mm wave distributed directional coupler made of the LRDW has also been extensively studied using the FDTD method. Results for the same coupler using an ideal design have also been presented. The discrepancy between FDTD results and ideal coupler ones is due to the parasitic

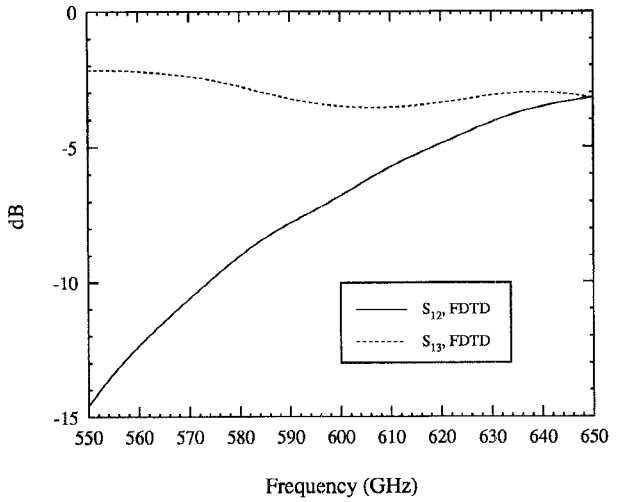

Fig. 15. Scattering parameters of the LRDW coupler obtained using FDTD. $S = 40\,\mu$m, $L = 80\,\mu$m, $d = 320\,\mu$m, $\theta = 26^o$.

effects of the junctions and radiation loss. A 3-dB coupler with a center frequency of 650 GHz and negligible radiation loss has been realized. The use of the FDTD method allows for the characterization of such components in a very wide frequency range. This paper shows that the FDTD technique can be used not only as an analysis method, but also as a design tool which can account for all the parasitic effects.

REFERENCES

[1] A. G. Engel, Jr. and L. P. B. Katehi, "Low-loss monolithic transmission lines for submillimeter and terahertz frequency applications," *IEEE Trans. Microwave Theory Tech.*, vol. 36, no. 11, pp. 1847–1854, Nov. 1991.

[2] S. Bhooshan and R. Mittra, "On the design of transitions between a metal and inverted strip dielectric waveguide for millimeter waves," *IEEE Trans. Microwave Theory Tech.*, vol. MTT-29, no. 3, pp. 263–265, Mar. 1981.

[3] J. Malherbe, J. Cloete, and I. Losch, "A transition from rectangular to nonradiating dielectric waveguide," *IEEE Trans. Microwave Theory Tech.*, vol. MTT-33, no. 6, pp. 539–543, June 1985.

[4] A. Engel, N. Dib, and L. Katehi, "Characterization of a shielded transition to a dielectric waveguide," *IEEE Trans. Microwave Theory Tech.*, vol 42, no. 5, pp. 847–854, May 1994.

[5] A. G. Engel, Jr. and L. P. B. Katehi, "On the analysis of a transition to a layered ridged dielectric waveguide," in *1992 IEEE MTT-S Int. Microwave Symp. Dig.*, pp. 983–986.

[6] R. Rudokas and T. Itoh, "Passive millimeter-wave IC components made of inverted strip dielectric waveguides," *IEEE Trans. Microwave Theory Tech.*, vol. MTT-24, no. 12, pp. 978–981, Dec. 1976.

[7] J. Miao and T. Itoh, "Hollow image guide and overlayed image guide coupler," *IEEE Trans. Microwave Theory Tech*, vol. MTT-30, no. 11, pp. 1826–1831, Nov. 1982.

[8] J. Rodriguez and A. Prieto, "Wide-band directional couplers in dielectric waveguide," *IEEE Trans. Microwave Theory Tech.*, vol. MTT-35, no. 8, pp 681–686, Aug. 1987.

[9] K. Solbach, "The measurement of the radiation losses in dielectric image line bends and the calculation of a minimum acceptable curvature radius," *IEEE Trans. Microwave Theory Tech.*, vol. MTT-27, no 1, pp. 51–53, Jan. 1979.

[10] K. Kunz and R Luebbers, *The Finite-Difference Time-Domain Method for Electromagnetics*. Boca Raton, FL: CRC, 1993.

[11] D. Sheen, S Ali, M. Abouzahra, and J. Kong, "Application of the three-dimensional finite-difference time-domain method to the analysis of planar microstrip circuits," *IEEE Trans. Microwave Theory Tech.*, vol. 38, no. 7, pp. 849–857, July 1990.

[12] L. Wu and H. Chang, "Analysis of dispersion and series gap discontinuity in shielded suspended striplines with substrate mounting grooves," *IEEE Trans. Microwave Theory Tech.*, vol. 40, no. 2, pp. 279–284, Feb. 1992.

[13] F. Moglie, T. Rozzi, and P Marcozzi, "Circuit modeling of waveguide discontinuities by FD-TD methods," *Proc. 1993 Eur. Microwave Conf*, pp. 668–669.

[14] K. Mei and J. Fang, "Superabsorption-A method to improve absorbing boundary conditions," *IEEE Trans. Antennas Propagat.*, vol. 40, no. 9, pp. 1001–1010, Sept. 1992.

[15] K. Solbach, "The calculation and measurement of the coupling properties of dielectric image lines of rectangular cross section," *IEEE Trans. Microwave Theory Tech.*, vol. MTT-27, no. 1, pp. 54–58, Jan. 1979.

[16] N. Dib and L. Katehi, "Analysis of the transition from rectangular waveguide to shielded dielectric image guide using the finite-difference time-domain method," *IEEE Microwave Guided Wave Lett.*, vol. 3, no. 9, pp 327–329, Sep 1993.

[17] G. Ponchak, N. Dib, and L. Katehi, "A novel transition between rectangular waveguide and layered ridge dielectric waveguide," in *Proc. 24th Eur. Microwave Conf.*, Sept. 1994, pp. 1933–1937.

[18] J. Yook, N. Dib, and L. Katehi, "Characterization of high frequency interconnects using finite-difference time-domain and finite element methods," *IEEE Trans. Microwave Theory Tech.*, vol. 42, no. 9, pp. 1727–1736, Sep. 1994.

Nihad Dib, photograph and biography not available at the time of publication.

Linda P. B. Katehi (S'81–M'84–SM'89–F'95), for a photograph and biography, see p. 3 of the January 1996 issue of this TRANSACTIONS.